IOP Publishing — Journal of Micromechanics and Microengineering
J. Micromech. Microeng. **18** (2008) 064008 (5pp) doi:10.1088/0960-1317/18/6/064008

Thermoelectric micro converters for cooling and energy-scavenging systems

L M Goncalves[1], C Couto[1], P Alpuim[2] and J H Correia[1]

[1] Department of Industrial Electronics, University of Minho, Campus de Azurém, 4800-058 Guimaraes, Portugal
[2] Department of Physics, University of Minho, Campus de Azurém, 4800-058 Guimaraes, Portugal

E-mail: lgoncalves@dei.uminho.pt

Received 10 December 2007, in final form 18 February 2008
Published 13 May 2008
Online at stacks.iop.org/JMM/18/064008

Abstract
This paper describes the fabrication process of thermoelectric microconverters, based on n-type bismuth telluride (Bi_2Te_3) and p-type antimony telluride (Sb_2Te_3) thin films. The films are fabricated by thermal co-evaporation with thermoelectric properties comparable to those reported for the same materials in bulk form (used in conventional macro-scale Peltier modules). The absolute value of the Seebeck coefficient in the range of 150–250 μV K^{-1} and an in-plane electrical resistivity of 7–15 $\mu\Omega$ m were obtained. The influence of fabrication parameters on thermoelectric properties is reported. The films were patterned by photolithography and wet-etching techniques, using HNO_3/HCl-based etchants. The influence of composition and concentration of etchants in the lithographic process is reported. A microcooler was fabricated.

(Some figures in this article are in colour only in the electronic version)

1. Introduction

Tellurium alloys (n-type Bi_2Te_3 and p-type Sb_2Te_3) are well-established thermoelectric materials for operation near room temperature, widely used in the thermoelectric industry (macro-scale conventional Peltier modules), since they have a high Seebeck coefficient, low electrical resistivity and a relatively low thermal conductivity.

The fabrication of efficient solid-state thermoelectric microdevices, for local cooling and thermoelectric energy scavenging, requires thin-film deposition processes, patterning and easy integration with a standard Si technology [1]. Thermoelectric energy-scavenging microsystems fabricated with tellurium alloys can power small electronic devices (up to units of miliWatt) under temperature differences bellow 10 °C. This type of energy converters can also be used in human-body power generators [2–4], to obtain energy from temperature differences between body (≈37 °C) and room temperatures. Peltier microcoolers can achieve temperature differences up to 60 °C, between hot and cold sides. Despite the range of exciting applications, only few approaches to manufacture thermoelectric devices with small dimensions were reported up to now [5–7]. Tentative deposition of thin films by direct evaporation of the bulk materials (Bi_2Te_3 and Sb_2Te_3) proved to be impossible due to the large differences in the vapour pressure of bismuth, antimony and tellurium, resulting in a compositional gradient along the film thickness [8]. Other techniques have been reported in the literature for the deposition of telluride thin films. Co-sputtering, electrochemical deposition, metal-organic chemical vapour deposition or flash evaporation are some examples.

Concerning the use of patterning techniques on thermoelectric films, few approaches have been reported in the literature. da Silva *et al* [6] uses lift-off, with SU-8 photoresist, to create vertical columns of thermoelectric materials. But due to the maximum working temperature of SU-8 photoresist (≈180 °C), thermoelectric properties of Bi_2Te_3 and Sb_2Te_3 films incorporated in the devices are worse than those obtained in bulk materials, since 200–300 °C of substrate temperature is required to fabricate high-quality thermoelectric films. Böttner *et al* [5] uses dry etching to pattern thermoelectric devices. Shafai [9] reports the patterning of Bi_2Te_3 films by wet etching but no details are given of the process.

In the present work, co-evaporation is applied in the fabrication of thermoelectric thin films, and the influence of growing parameters is studied in detail. A low-cost wet-etching technique is presented in detail, imposing no temperature limits on film deposition.

 © 2008 IOP Publishing Ltd Printed in the UK

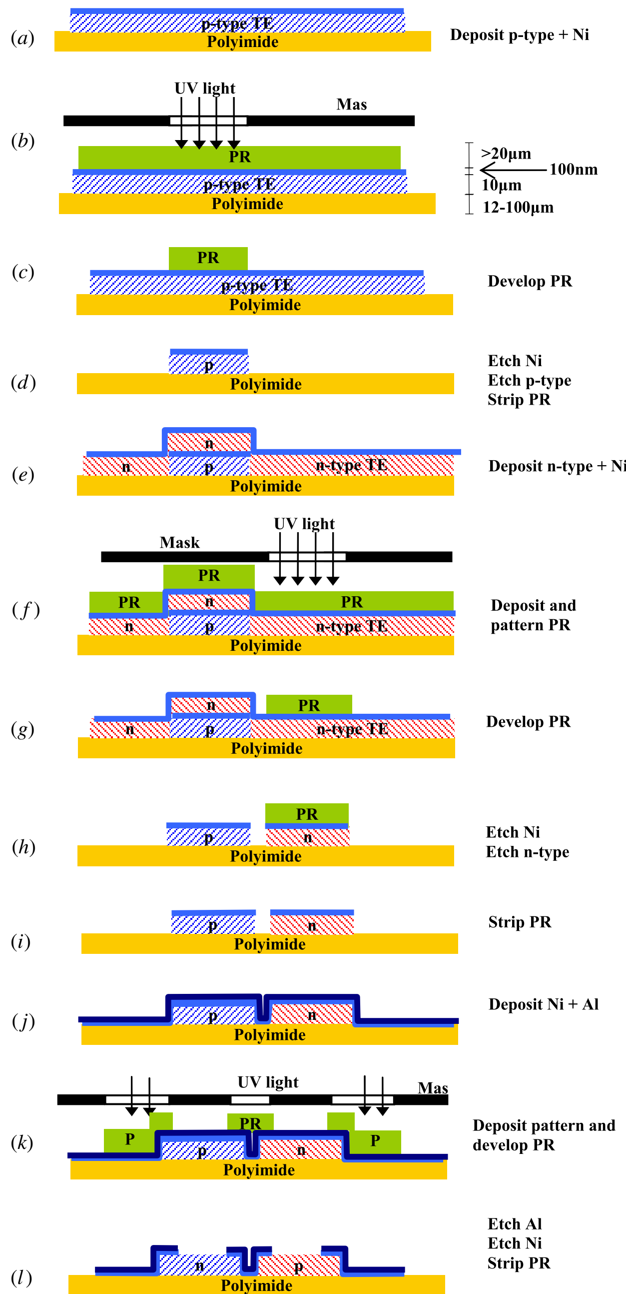

Figure 1. Fabrication steps of thermoelectric converters.

2. Fabrication process

Figure 1 shows the fabrication process of thermoelectric converters. The p-type Sb_2Te_3 film is deposited by thermal co-evaporation followed by a thin layer (100 nm) of nickel (a). The thin layers of nickel are used to avoid diffusion of the thermoelectric material into the next deposited layers. Photoresist (PR) is spun and p-type elements are patterned by photolithography (b), (c). Nickel is etched in a chromium etchant (Transene 1020), a thermoelectric film is patterned by wet etching in HNO_3:HCl bath (d) and PR is removed. The n-type film is then deposited by co-evaporation, followed by a 100 nm nickel layer (e). PR is applied and patterned by photolithography for n-type element definition (f), (g). Nickel is etched in a chromium etchant (Transene 1020), the n-type film is etched in HNO_3 (h) and PR is removed (i). Contacts are deposited, starting with a 100 nm layer of nickel, followed by 1 μm of aluminium (j). PR is spun and contacts patterned by photolithography (k). Nickel is etched in a chromium etchant (Transene 1020), and aluminium is with a standard aluminium etchant (Transene type A). PR is removed (l). A protective layer of Si_3N_4 can also be deposited by low-temperature hot-wire chemical vapour deposition (HW-CVD) and patterned if required, depending on the application.

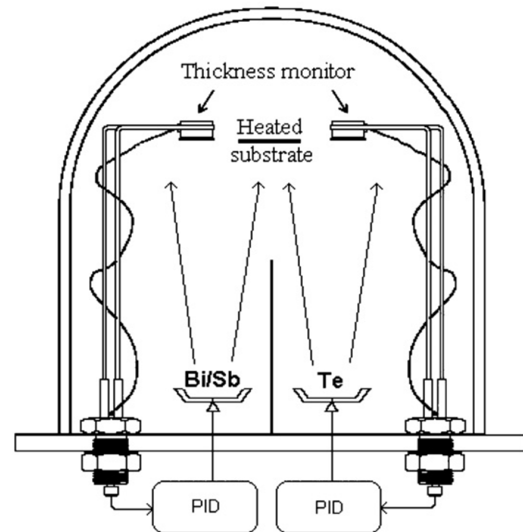

Figure 2. Thermal co-evaporation system.

2.1. Thin-film deposition

Thermoelectric films were fabricated by the thermal co-evaporation technique (figure 2) in a high-vacuum chamber (base pressure $\sim 1 \times 10^{-6}$ Torr) [10]. Two large molybdenum boats (baffled boxes, 4 cm^3 in volume) are used at the same time, one for each of the elementary materials required to produce the desired compound. The power applied to each boat is controlled independently, using two computed proportional-integral derivative (PID) controllers to maintain the deposition rate at user-defined constant values, during the deposition process. Two thickness monitors (quartz crystal oscillators) are carefully placed inside the chamber in such a way that each of them receives material only from the boat it is monitoring. To prevent mixing of both materials to occur at the quartz crystal sensors, a metal sheet is placed between the two boats. Substrates are heated to the temperature set point (T_{sub}) in the range 150–270 °C [11].

Tables 1 and 2 present thermoelectric properties of selected films. Equations (1) and (2) are used to calculate the power factor, PF, and the figure of merit, ZT:

$$PF = \alpha^2/\rho \tag{1}$$

$$ZT = \frac{\alpha^2}{\rho\lambda}T \tag{2}$$

Table 1. Properties of selected Bi_2Te_3 films in this work and from the literature.

Film	Temp T_{sub} °C	$R = F_{Te}/F_{Bi}$	α (μV K^{-1})	ρ ($\mu\Omega$ m)	PF $\times 10^{-3}$ (WK^{-2} m^{-1})	ZT@300 K
#302A	160	1.6	−74	5.7	0.96	0.19
#C36	190	1.7	−180	16.6	1.95	0.4
#267A	230	2.1	−156	11.3	2.16	0.43
#267D	230	3.0	−152	13.4	1.72	0.34
#273C	270	3.2	−248	12.6	4.87	0.97
#281D	270	3.9	−220	10.6	4.57	0.91
Luci [6]	260	–	−228	28.3	1.84	–
Zou [13]	260	–	−228	13.0	4.0	–
Shafai [9]	–	–	−187	11.5	3.04	–

Table 2. Properties of selected Sb_2Te_3 films in this work and from the literature.

Film	Temp T_{sub} °C	$R = F_{Te}/F_{Sb}$	α (μV °C^{-1})	ρ ($\mu\Omega$ m)	PF $\times$ 10^{-3} W K^{-2} m^{-1}	ZT@300 K
#195C	150	1.47	91	7.6	1.09	0.22
#305A	150	1.67	140	14.0	1.40	0.28
#306A	220	2.50	156	9.2	2.66	0.53
#306D	220	3.18	188	12.6	2.81	0.56
Luci [6]	270	–	149	12.5	1.78	–
Zou [13]	230	–	171	10.4	2.81	–

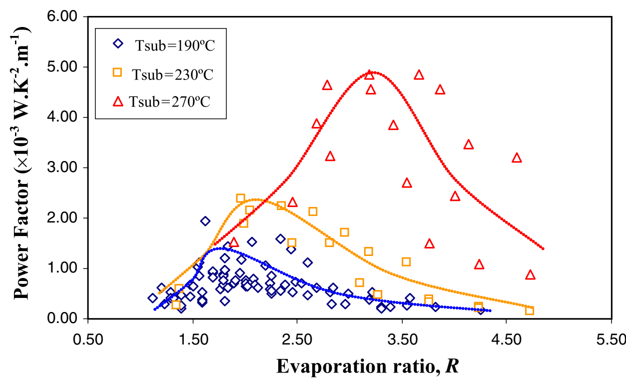

Figure 3. Power factor of Bi_2Te_3 thin films as a function of the Te/Bi evaporation flow rate ratio, *R*.

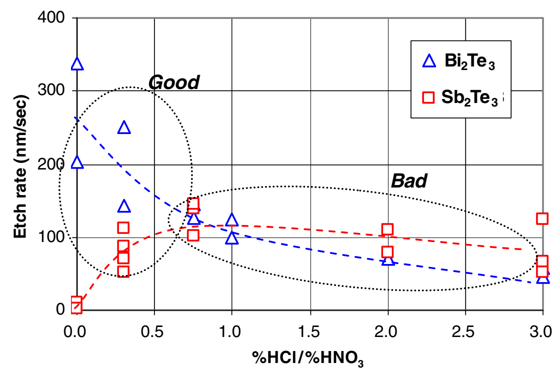

Figure 5. Etch rate of Bi_2Te_3 and Sb_2Te_3 films in $(1-x)HNO_3$:$(x)HCl$ solution (diluted 70% in water, in volume).

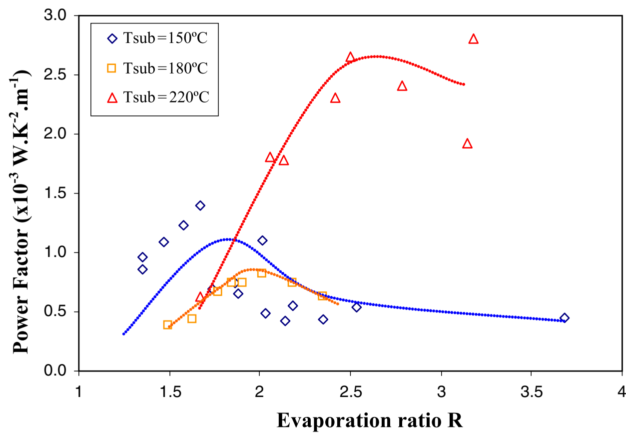

Figure 4. Power factor of Sb_2Te_3 thin films as a function of the Te/Sb evaporation flow rate ratio, *R*.

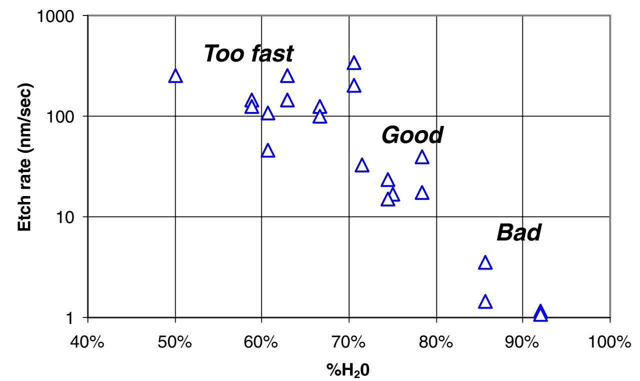

Figure 6. Etch rate of a Bi_2Te_3 film in 10:3 HNO_3:HCl solution, as a function of dilution in water (in volume).

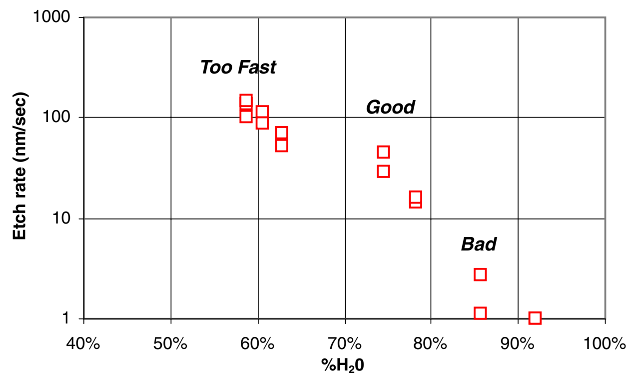

Figure 7. Etch rate of a Sb_2Te_3 film in 10:1 HNO_3:HCl solution, as a function of dilution in water (in volume).

where α is the Seebeck coefficient in VK^{-1}, ρ is electrical resistivity in Ω m, λ is the thermal conductivity in $Wm^{-1}\ K^{-1}$ and T is the temperature in K. The thermal conductivity was measured using the method described by Völklein [12] and values of 1.3 $Wm^{-1}\ K^{-1}$ and 1.8 $Wm^{-1}\ K^{-1}$ were obtained in Bi_2Te_3 and Sb_2Te_3 films (deposited as conditions to obtain maximum power factor, presented in figures 3 and 4).

Figures 3 and 4 show the influence of the evaporation rate of each material on the thermoelectric properties of the compounds. The evaporation flow rate ratio ($R = Fr_{Te}/Fr_{Bi,Sb}$) is defined as the amount (in volume of the deposited film) of Te divided by the amount of Bi (or Sb) that arrives the substrate during deposition. The highest thermoelectric power factor was obtained with a Bi (or Sb) evaporation rate of 2 $Ås^{-1}$ and a Te evaporation rate of 6–7 $Ås^{-1}$ ($R = 3$–3.5). Optimized T_{sub} was ≈270 °C for Bi_2Te_3 and ≈220 °C for Sb_2Te_3 films [10]. All films were deposited on a 25 μm thick kapton polyimide foil.

2.2. Patterning

Thermoelectric Bi_2Te_3 and Sb_2Te_3 thin films (1 μm thick) were deposited on the kapton substrate. Transene's PKP negative photoresist was applied on the surface and test structures were patterned by wet etching in the HNO_3:HCl:H_2O etchant (pure HNO_3 and 37% HCl dil. in water). Figure 5 shows the influence of the etchant composition on the etch rates. Higher per cent of HCl (%HCl/%HNO_3 > 0.5) induces cracking of the film and peeling occurs. Figure 6 shows the influence of etchant dilution (in water) on the etch rate of Bi_2Te_3 films. Dilution above 85% cause peeling to occur. For dilutions below 65%, etching occurs in a too fast manner and the end of the process is difficult to detect. Best results are obtained with the etchant composition in the range of 10:0:25–10:5:40 HNO_3:HCl:H_2O.

Figure 5 also shows the influence of the etchant composition on the etching process of Sb_2Te_3 films. Cracking and peeling of the film occur when a high percentage of HCl is present in the etchant (%HCl/%HNO_3 > 0.5), as was observed for the Bi_2Te_3 films. The etch rate of the Sb_2Te_3 films in diluted HNO_3 was about 50 times smaller than the etch rate of Bi_2Te_3 films in the same etchant. This is important in terms of the selectivity of the process in the presence of both materials. The influence of etchant dilution in the etch rates of Sb_2Te_3 films is shown in figure 7. Best results are obtained with the etchant of composition in the range 10:1:20 to 10:6:40 HNO_3:HCl:H_2O.

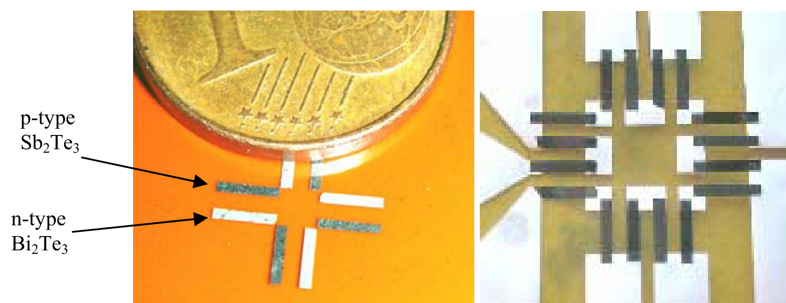

Figure 8. (Left) Photo of n-type and p-type elements, before deposition of top contacts. (Right) Photo of a microcooler with eight pairs of thermoelectric elements, fabricated with bottom contacts.

Table 3. Summary of etch rates.

Etchant	Material Bi_2Te_3	Sb_2Te_3	Aluminium	Nickel
Al— Transene type A	8 Å s^{-1}	5 Å s^{-1}	10–80 Å s^{-1}	<0.1 Å s^{-1}
Cr—Transene 1020	≈20 Å s^{-1}	<1 Å s^{-1}	–	10–40 Å s^{-1}
3HNO3:1HCl (dil 70% H20)	2000 Å s^{-1}	800 Å s^{-1}	<2 Å s^{-1}	<0.2 Å s^{-1}
HNO3 (dil 70% H20)	2500 Å s^{-1}	50 Å s^{-1}	< 0.1 Å s^{-1}	< 0.1 Å s^{-1}

For chromium and aluminium films using the same etching solutions used for tellurium compounds, etch rates below 0.2 nm s^{-1} were observed regardless of the etchant composition used. Both Bi_2Te_3 and Sb_2Te_3 are slightly etched (<2 nm s^{-1}) by an aluminium etchant (16:1:1:2 phosphoric acid, nitric acid, acetic acid and water) or a Cr etchant (Transene 1020). Table 3 gathers together all relevant etch rates.

A planar thermoelectric converter was fabricated on top of a 100 μm thickness kapton foil. Contacts can be deposited on top or bottom of the thermoelectric films (figure 8). Since Bi_2Te_3 and Sb_2Te_3 adhesion is higher on kapton films than on nickel metal pads, the use of top contacts process (as presented in figure 1) avoids the need of depositing additional layers to promote the adhesion of thermoelectric films.

3. Conclusions

Thermoelectric thin films with high figure of merit (≈0.97 in n-type film and ≈0.56 in p-type film) were obtained by thermal co-evaporation. The best film depositions were achieved with a Bi (Sb) evaporation rate of 2 Ås^{-1} and a Te evaporation rate of 6–7 Ås^{-1}. The substrate was heated between the temperature of 220 and 270 °C respectively for optimized Bi_2Te_3 and Sb_2Te_3 film depositions. The influence of the deposition parameters in the thermoelectric properties of the films was reported. Films were patterned by wet etching in HNO_3:HCl:H_2O and the influence of the etchant composition in the etch rate and pattern quality was investigated. The optimized wet-etching results (with an etch rate of 100–200 nm s^{-1}) were obtained with 10:3:30 HNO_3:HCl:H_2O. The etch rate below 0.2 nm s^{-1} was observed in aluminium and chromium films, allowing a selectivity higher than 1000. Bi_2Te_3 can also be etched in the 30% HNO_3 etchant, with a selectivity higher than 50 to Sb_2Te_3 films. A thin layer of nickel prevented diffusion between adjacent layers of thermoelectric materials and improved the contact resistance. The fabrication process described was applied in the thermoelectric microcooler implementation. Wet etching is a low-cost technique (comparing with ion etching) and imposes no limit on substrate temperature during the deposition (unlike lift-off process that is limited by the photoresist working temperature).

Acknowledgments

This work was supported by ADI (MPYROM), FCT/PTDC/EEA-ENE/66855/2006 and FCT (SFRH/BD/18142/2004). Thermal conductivity was measured by Professor Völklein in FW Wiesbaden, Germany.

References

[1] Roundy S, Steingart D, Frechette L, Wright P and Rabaey J 2004 Power sources for wireless sensor networks *1st European Workshop on Wireless Sensor Networks (Berlin, 19–21 Jan. 2004)*

[2] Shenck N S and Paradiso J A 2001 Energy scavenging with shoe-mounted piezoelectrics *IEEE Micro* **21** 30–41

[3] Tashiro R, Kabei N, Katayama K, Ishizuka Y, Tsuboi R and Tsuchiya K 2000 Development of an electrostatic generator that harnesses the motion of a living body *Japan Soc. Mech. Eng. Int. J.* **43** 916–22

[4] Qu W, Plotner M and Fischer W J 2001 Microfabrication of thermoelectric generators on flexible foil substrates as a power source for autonomous microsystems *J. Micromech. Microeng.* **11** 146–52

[5] Böttner Harald *et al* 2004 New thermoelectric components using microsystem technologies *J. Microelectromech. Syst.* **13** 414–20

[6] da Silva L W and Kaviany M 2005 Fabrication and measured performance of a first-generation microthermoelectric cooler *J. Microelectromech. Syst.* **14** 1110

[7] Venkatasubramanian R, Siivola E, Colpitts T and O'Quinn B 2001 Thin-film thermoelectric devices with high room temperature figures of merit *Nature* **413** 597

[8] da Silva L W and Kaviany M 2002 Miniaturized thermoelectric cooler *2002 ASME '02 (New Orleans, USA, 17–22 Nov. 2002)*

[9] Shafai C 1998 *Fabrication of a Micro-Peltier Device* (National Library of Canada) p 76

[10] Goncalves L M, Couto C, Correia J H, Alpuim P, Min Gao and Rowe D M 2006 Optimization of thermoelectric thin films deposited by co-evaporation on plastic substrates, *ECT 2006 (Cardiff, UK, 2006)*

[11] Goncalves L M, Couto C, Correia J H, Alpuim P, Min G and Rowe D M 2006 Flexible thin-film planar Peltier microcooler *ICT '06 (Vienna, Austria, 2006)*

[12] Völklein F 2000 *Proc. Symp. on Microtechnology in Metrology and Metrology in Microsystems (Delft, The Netherlands)*

[13] Zou H, Rowe D M and Min G 2001 Growth of p- and n-type bismuth telluride thin films by co-evaporation *J. Cryst. Growth* **222** 82–7